JOTCS A
Journal of the Turkish Chemical Society
Section: A
Chemistry
TURKISH CHEMICAL SOCIETY

Mechanical, Optical, and Thermal Properties of SnS_2-Filled PVA Composites

Volkan Uğraşkan[1*]

[1]Yildiz Technical University, Chemistry Department, Istanbul, 34220, Turkey.

Abstract: The effects of tin disulfide (SnS_2) addition on the mechanical, thermal, and optical characteristics of polyvinyl alcohol (PVA) were determined in this study. The solvent-casting approach was used to create composite films with varying SnS_2 weight ratios. Mechanical testing revealed that the addition of SnS_2 raised the tensile strength (TS) of the virgin PVA from 32.10 MPa to 47.50 MPa, while the elongation at break (EB) increased from 78.40% to 108.80%. Optical investigations revealed that PVA and SnS_2 had intermolecular interactions. Furthermore, the contribution of SnS_2 resulted in a drop in energy bandwidth from 5.310 eV to 4.821 eV. Thermal investigations revealed that PVA/SnS_2 had greater stability than the virgin polymer. Given the data obtained, it was obtained that the addition of SnS_2 simultaneously enhanced the mechanical, thermal, and optical properties of PVA.

Keywords: Polyvinyl alcohol, tin disulfide, polymer, composite.

Submitted: July 8, 2023. **Accepted:** January 23, 2024.

Cite this: Uğraşkan V. Mechanical, Optical, and Thermal Properties of SnS_2-Filled PVA Composites. JOTCSA. 2024;11(2):557-64.

DOI: https://doi.org/10.18596/jotcsa.1324711

***Corresponding author's E-mail:** ugraskan@yildiz.edu.tr

1. INTRODUCTION

There has been a recent interest in thermoplastic composites filled with various fillers that are used to improve the physicomechanical properties and provide desirable properties to composites used in food packaging, drug delivery, automation, aerospace, textile, and so on applications (1). These composites have the features of organic polymers, such as lightweight and good moldability, as well as the inorganic materials' high strength, thermal stability, and chemical resistance (2).

Polyvinyl alcohol (PVA) is a semi-crystalline organic polymer produced by vinyl acetate polymerization. Because of its excellent film-forming, adhesion, emulsification, and chemical stability, it could potentially be employed in a variety of pharmaceutical, cosmetic, or biological applications such as drug administration, tissue engineering, tissue regeneration, or replacement. It should be noted that PVA is difficult to melt because of its strong inter/intra hydrogen bonding, yet the many hydroxyl groups in the molecular structure supply PVA with exceptional water solubility, making it ideal for casting (3-5). Furthermore, virgin PVA films display low dielectric permittivity and weak conductivity behavior across a wide frequency range, proving their suitability as low-dielectric ecologically friendly, transparent compounds. The customizable usability of these polymers' composites with diverse fillers has proven them as particularly suitable for the construction of a wide range of flexible and lightweight biodegradable microelectronic, organoelectronic, and optoelectronic technologies (6).

Tin disulfide (SnS_2) is a 2.2 eV moderate bandgap CdI_2-type multilayer semiconducting material. It has recently piqued the interest of researchers for use in a variety of applications such as lithium batteries, pigments, gas sensors, photoconductors, solar cells, optoelectronics, photoluminescence, and so on due to its plentiful source components, simple synthesis, cost-effectiveness, non-toxicity, strong stability, and comparatively strong visible-light photocatalytic activity (7-10). However, there is no study reported on the mechanical properties of SnS_2 and its composites in the literature.

In this work, the mechanical, optical, electrical, and thermal properties of SnS_2-filled PVA composites were examined.

2. EXPERIMENTAL SECTION

2.1. Materials

PVA (Mowiol 40-88), tin (II) chloride dehydrate (98%), thiourea (≥99.0%), and ethylene glycol (99.8%) were purchased from Sigma Aldrich, Germany.

2.2. Synthesis of SnS_2

The synthesis of SnS_2 was carried out as described in the literature (8). To begin, tin(II) chloride dehydrate and thiourea was grounded in a mortar at a mole ratio of 0.2:0.5. The powder combination was then transferred to a porcelain crucible and heated at 170 °C for 2 h. Lastly, the resulting yellowish SnS_2 was rinsed with distilled water to eliminate impurities and dried overnight in an oven at 90 °C.

2.3. Preparation of The Composite Films

PVA/SnS_2 composites were produced by incorporating several weight ratios of SnS_2 such as 0.5%, 1%, 3%, 5%, 7%, and 10% into a 10% w/v PVA solution. The combinations were then cast on glass templates. The composite films were formed following drying at 60 °C under vacuum.

2.4. Characterization

The instruments used in this study are listed in Table 1.

Table 1: The instruments used in this study.

Instruments	Model
FTIR-ATR	Nicolet IS10 Thermo FTIR
SEM	Zeiss EVO LS10
XRD	Panalytical Empyrean
UV-vis	Shimadzu UV2600
TGA and DSC	NETZSCH STA 449F3
Tensile tests	ZONHOW, DZ-106

3. RESULTS AND DISCUSSION

XRD spectra of the virgin PVA, SnS_2, and PVA/SnS_2 containing 3% SnS_2 were given in Fig. 1. The pattern of the virgin PVA film displayed two peaks at 19.5° and 41.4°, which correspond to the semi-crystalline structure kept together by intramolecular and intermolecular H-bonding (11) (Fig. 1a). The diffraction pattern's reflections are all well-matched with characteristic SnS_2 crystals and showed the hexagonal SnS_2 phase. The acquired XRD results are consistent with the literature (JCPDPS card no. 22-0951) (7). In the pattern of the PVA/SnS_2, no significant change was observed compared to the virgin PVA, which was due to the homogenous distribution of SnS_2 particles in the composite structure (12).

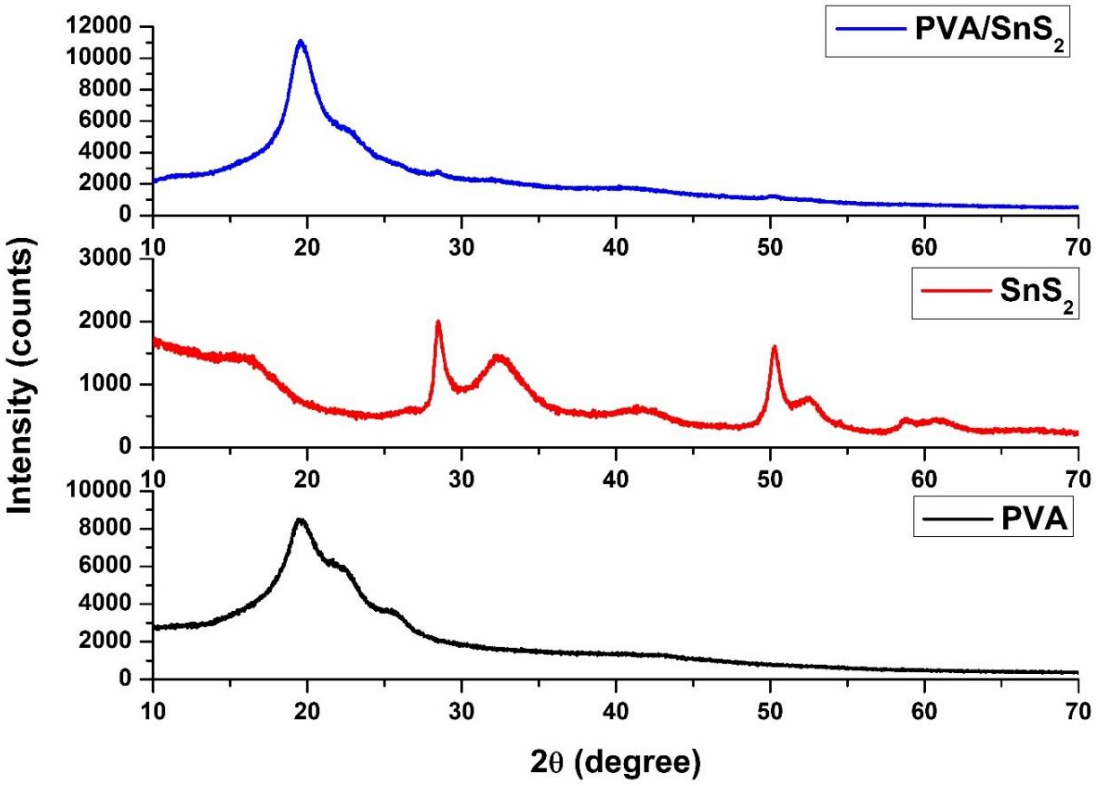

Figure 1: XRD patterns of the virgin PVA, SnS_2, and PVA/SnS_2 containing 3% SnS_2.

Fig. 2 showed the SEM images of SnS_2, and a cross-sectional view of the films of the virgin PVA, and PVA/SnS_2 containing 3% SnS_2. It was observed that the virgin PVA film had a smooth surface, while the composite surface was rough. Additionally, the homogenous distribution of the SnS_2 particles without any significant agglomeration in the composite structure was observed (Fig. 2a, c, d). The micrograph of SnS_2 revealed the porous flower-like hierarchical structures formed by interpenetrated sheets (8).

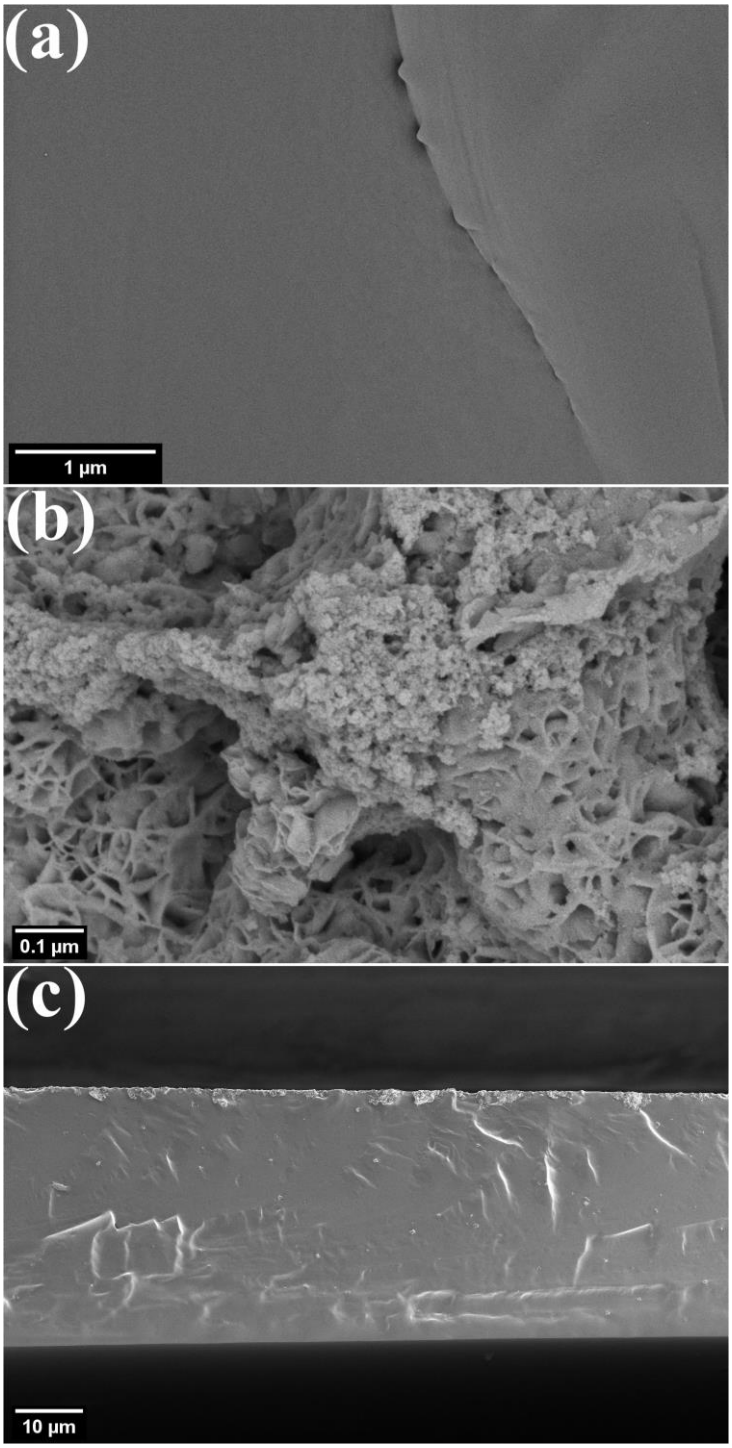

Figure 2: SEM images of the samples; cross-sectional view of the virgin PVA film (a), SnS_2 (b), cross-sectional view of the PVA/SnS_2 containing 3% SnS_2.

FTIR-ATR spectra of the virgin PVA, SnS_2, and PVA/SnS_2 containing 3% SnS_2 were given in Fig. 3 whereas the peak assignments were given in Table 2. For the PVA/SnS_2, a spectrum similar to that of virgin PVA was obtained, with the peak observed at 1628 cm^{-1} originating from SnS_2. Additionally, shifts in peak values were observed, which were attributed to the interaction of the SnS_2 particles with the PVA matrix.

UV-vis spectra of the virgin PVA and PVA/SnS_2 containing different weight ratios of SnS_2 were illustrated in Fig. 4. The virgin PVA exhibited a peak at 277 nm, which corresponded to π-π* transitions in the polymer backbone. In addition, a significant decrease in absorbance is noticed in the 200-240 nm range, which is related to the sample's band gap, suggesting the semi-crystalline structure of PVA as revealed by XRD analysis (14). The spectra of the PVA/SnS_2 were identical to those of the virgin PVA, however, the peaks corresponding to the π-π* transitions moved to higher wavelengths. The establishment of a strong intermolecular interaction between the SnS_2 particles and the polar unit of PVA caused a shift in the peak locations of PVA/SnS_2 to the higher wavelengths (15).

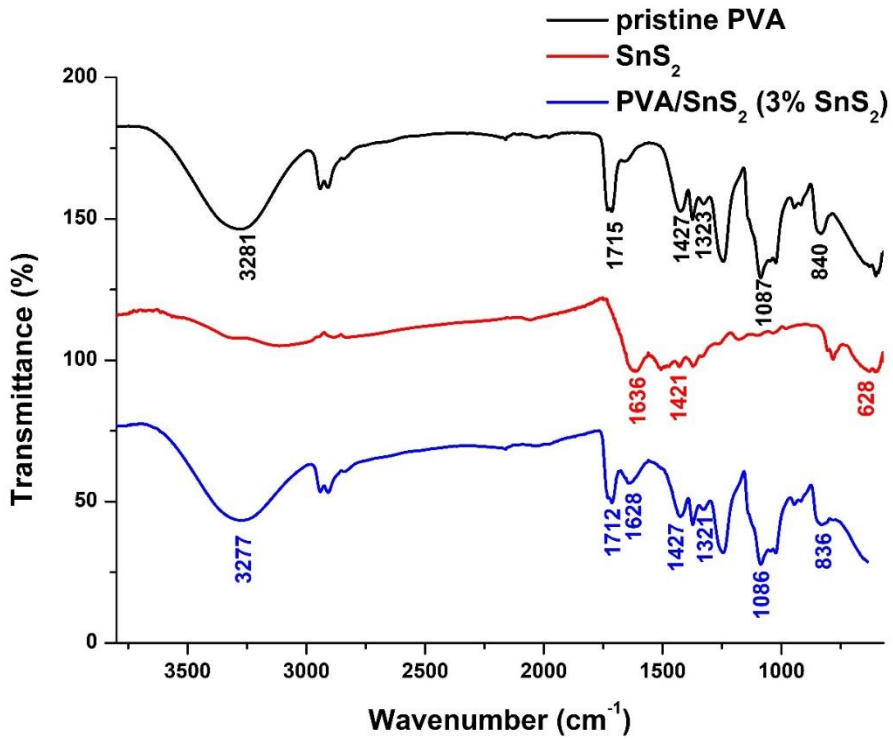

Figure 3: FTIR-ATR spectra of the virgin PVA, SnS_2, and PVA/SnS_2 containing 3% SnS_2.

Table 2: The FTIR-ATR data of the samples [7] [13].

Wavenumber (cm^{-1})	Functional group
3281	O-H stretchings
1715	C=O stretchings
1427	C-H bending
1323	C-H deformation
1087	C-O stretchings
840	C-C stretchings
1636	C–H stretchings
1421	C–O stretchings
628	Sn–S band

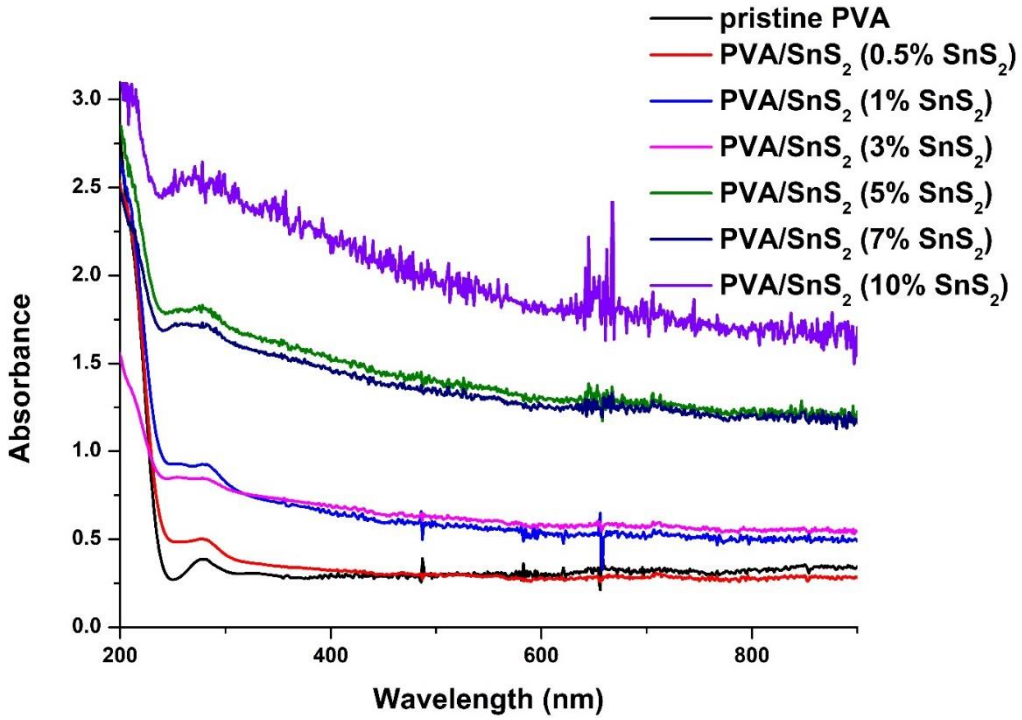

Figure 4: UV-VIS spectra of the virgin PVA, SnS_2, and PVA/SnS_2.

Knowing the absorption coefficients would allow you to calculate the optical energy band gaps (E_g), which are the most significant characteristics of organic and inorganic materials. The Tauc relation is utilized to calculate the films' energy band gap:

$$(\alpha h\nu) = B(h\nu - E_g)^{1/n}$$

where 1/n defines the type of electronic transition and is related to the density of state distribution. B is a constant, connected to the probability of transition. Following that, optical band gaps were calculated by graphing $(\alpha h\nu)^2$ against $(h\nu)$. The energy bandwidth of the composites reduced from 5.310 to 4.767 eV when compared to pristine PVA film, indicating that SnS_2 might raise the amount of energy states between PVA's valence and conduction bands, leading to a change in the electronic structure of the PVA matrix (Fig. 5). The change in the optical bandgap is caused by the localized electronic states in the band gaps of PVA created by SnS_2 as trapping and recombination centers (16).

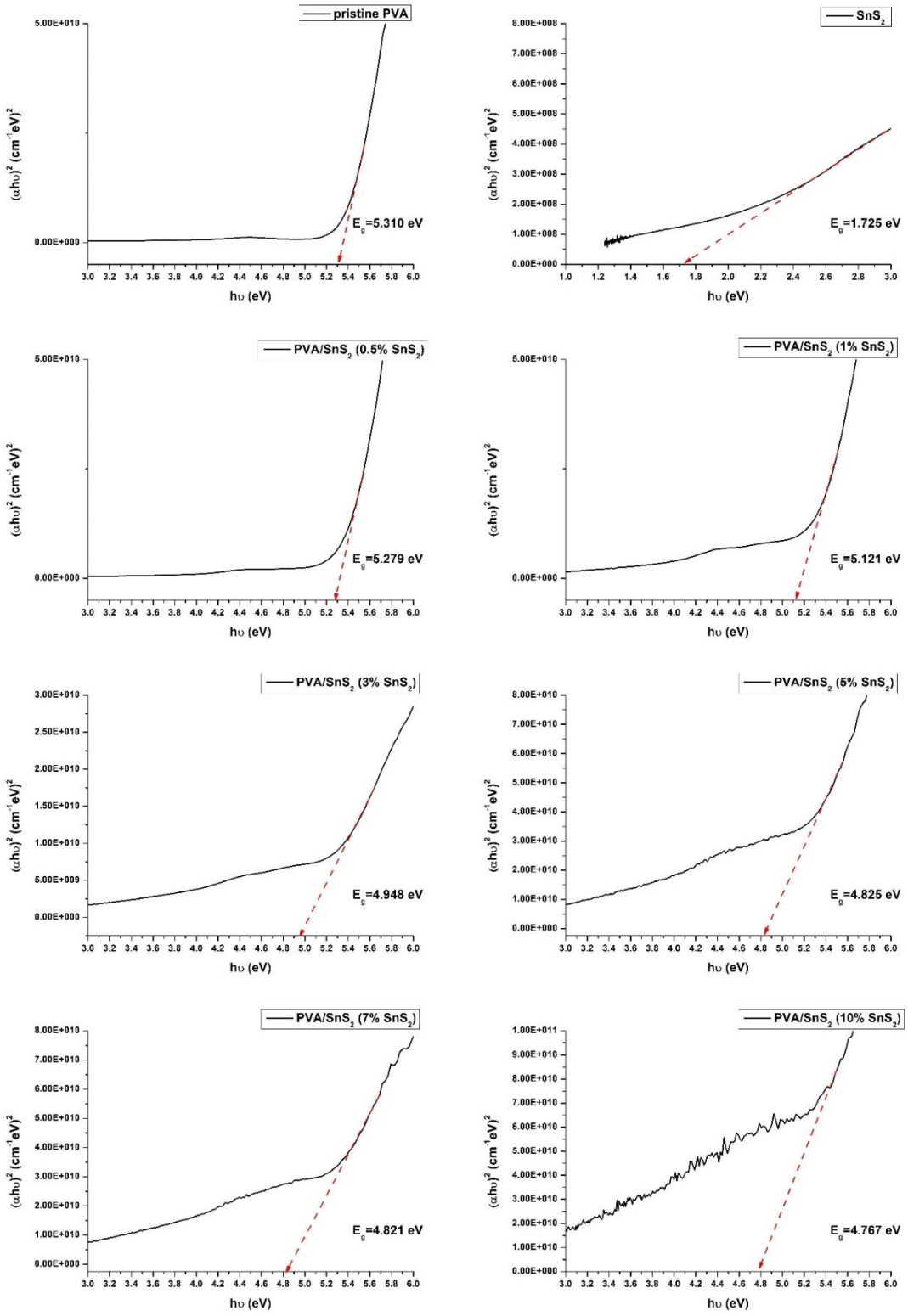

Figure 5: $(\alpha h\nu)^2$ against $(h\nu)$ plots of the pristine PVA, SnS_2, and PVA/SnS_2 composites.

The TGA spectrum of the virgin PVA and PVA/SnS_2 containing 3% SnS_2 were shown in Fig. 6. The weight losses observed in all samples below 100 °C indicated the removal of the absorbed water molecules from the structure (17). SnS_2 was thermally stable and showed a 7.2 wt% weight loss between 260 and 460 °C. The spectra of the virgin PVA and PVA/SnS_2 revealed a two-stage decomposition trend. While the samples began to deteriorate at roughly 260 °C, they were completely decomposed at around 460 °C. Additionally, the breakdown temperature of PVA/SnS_2 (270 °C) is greater than that of virgin PVA (260 °C). Besides, according to the DSC data, it was observed that the melting temperature of the virgin PVA increased from 187.5 °C to 189.1 °C with the addition of 3% SnS_2. The rise in the thermal stability was ascribed to SnS_2 particles' superior temperature stability and interfacial interactions with the PVA matrix (18).

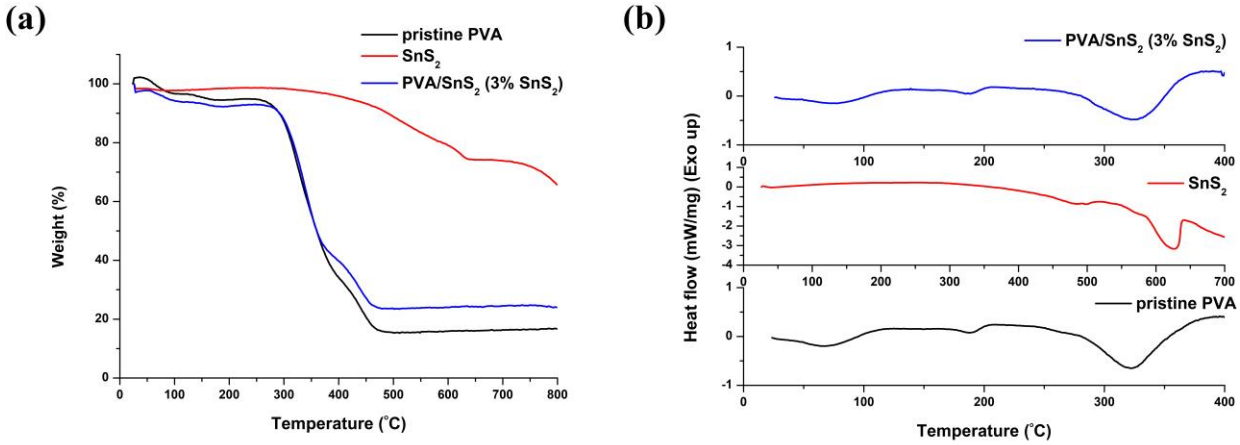

Figure 6: TGA spectra (a) and DSC curves (b) of the virgin PVA, SnS_2, and PVA/SnS_2 containing 3% SnS_2.

Fig. 7 depicts the stress-strain curves of the virgin PVA and PVA/SnS_2, whereas Table 3 lists the TS, Young's modulus, and EB. Tensile testing revealed that the virgin PVA's TS increased from 32.10 MPa to 47.50 MPa with the addition of 3% SnS_2. The composites demonstrated linear stress-strain behavior up to failure and plastic deformation, as well as equivalent curve morphologies for plain and nanofiller composites (19). Additionally, the simultaneous enhancement in the tensile strength and elongation was ascribed to the homogeneous dispersion of SnS_2 particles in the PVA/SnS_2 structure (20).

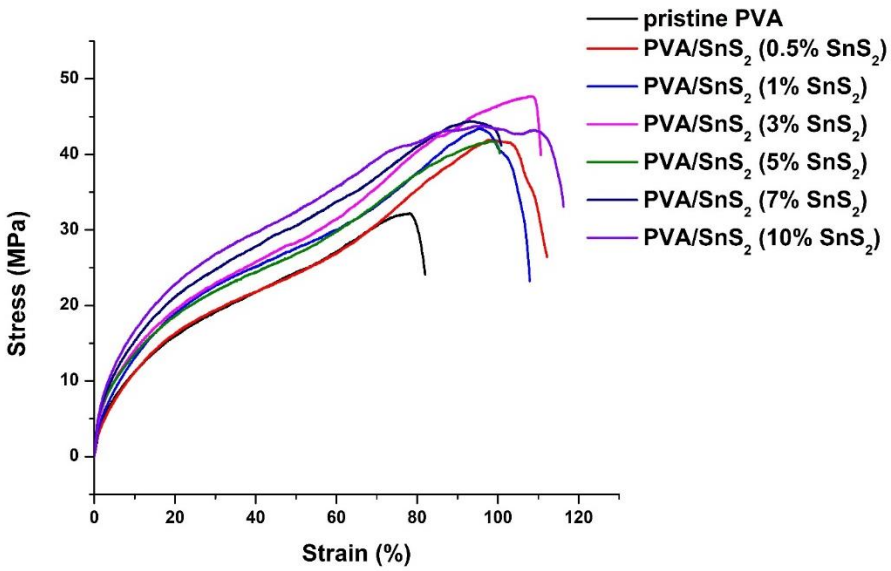

Figure 7: Stress-strain curves of the virgin PVA, SnS_2, and PVA/SnS_2.

Table 3: Tensile properties of the virgin PVA and PVA/SnS_2 films.

Sample	TS (MPa)	EB (%)	Young Modulus (GPa)
Virgin PVA	32.10	78.40	1.80
PVA/SnS_2 (0.5% SnS_2)	42.00	97.20	3.01
PVA/SnS_2 (1% SnS_2)	43.60	95.80	3.04
PVA/SnS_2 (3% SnS_2)	47.50	108.80	3.42
PVA/SnS_2 (5% SnS_2)	42.55	99.13	2.78
PVA/SnS_2 (7% SnS_2)	44.50	92.32	3.11
PVA/SnS_2 (10% SnS_2)	43.56	94.86	3.86

4. CONCLUSION

The mechanical, thermal, and optical features of SnS_2-filled PVA composites were examined in this work. Firstly, SnS_2 was synthesized, and then composite films with varied SnS_2 weight ratios were made using the solvent-casting process. Mechanical testing revealed that the addition of SnS_2 raised the TS of the virgin PVA from 32.10 MPa to 47.50 MPa, while the EB increased from 78.40% to 108.80%. Optical investigations revealed that the intermolecular interactions between PVA and SnS_2. Thermal investigations revealed that PVA/SnS_2 are more stable than virgin PVA.

5. CONFLICT OF INTEREST

The authors declare that they have no conflict of interest.

7. REFERENCES

1. Kohli D, Garg S, Jana AK. Physical, mechanical, optical and biodegradability properties of polyvinyl alcohol/cellulose nanofibrils/kaolinite clay-based hybrid composite films. Indian Chem Eng [Internet]. 2021 Jan 1;63(1):62–74. Available from: <URL>.

2. Chen T, Wu Z, Wei W, Xie Y, Wang X (Alice), Niu M, et al. Hybrid composites of polyvinyl alcohol (PVA)/Si–Al for improving the properties of ultra-low density fiberboard (ULDF). RSC Adv [Internet]. 2016;6(25):20706–12. Available from: <URL>.

3. Cavalu S, Fritea L, Brocks M, Barbaro K, Murvai G, Costea TO, et al. Novel Hybrid Composites Based on PVA/SeTiO$_2$ Nanoparticles and Natural Hydroxyapatite for Orthopedic Applications: Correlations between Structural, Morphological and Biocompatibility Properties. Materials (Basel) [Internet]. 2020 May 1;13(9):2077. Available from: <URL>.

4. Rathinavel S, Saravanakumar SS. Development and Analysis of Silver Nano Particle Influenced PVA/Natural Particulate Hybrid Composites with Thermo-Mechanical Properties. J Polym Environ [Internet]. 2021 Jun 2;29(6):1894–907. Available from: <URL>.

5. Yao Y, Jin S, Wang M, Gao F, Xu B, Lv X, et al. MXene hybrid polyvinyl alcohol flexible composite films for electromagnetic interference shielding. Appl Surf Sci [Internet]. 2022 Mar;578:152007. Available from: <URL>.

6. Sengwa RJ, Dhatarwal P. Nanofiller concentration-dependent appreciably tailorable and multifunctional properties of (PVP/PVA)/SnO_2 nanocomposites for advanced flexible device technologies. J Mater Sci Mater Electron [Internet]. 2021 Apr 13;32(7):9661–74. Available from: <URL>.

7. Umar A, Akhtar MS, Dar GN, Abaker M, Al-Hajry A, Baskoutas S. Visible-light-driven photocatalytic and chemical sensing properties of SnS_2 nanoflakes. Talanta [Internet]. 2013 Sep;114:183–90. Available from: <URL>.

8. Wei H, Hou C, Zhang Y, Nan Z. Scalable low temperature in air solid phase synthesis of porous flower-like hierarchical nanostructure SnS_2 with superior performance in the adsorption and photocatalytic reduction of aqueous Cr(VI). Sep Purif Technol [Internet]. 2017 Dec;189:153–61. Available from: <URL>.

9. Kiruthigaa G, Manoharan C, Raju C, Dhanapandian S, Thanikachalam V. Synthesis and spectroscopic analysis of undoped and Zn doped SnS_2 nanostructure by solid state reaction method. Mater Sci Semicond Process [Internet]. 2014 Oct;26:533–9. Available from: <URL>.

10. Kiruthigaa G, Manoharan C, Raju C, Jayabharathi J, Dhanapandian S. Solid state synthesis and spectral investigations of nanostructure SnS_2. Spectrochim Acta Part A Mol Biomol Spectrosc [Internet]. 2014 Aug;129:415–20. Available from: <URL>.

11. Aziz S, Abdulwahid R, Rasheed M, Abdullah O, Ahmed H. Polymer Blending as a Novel Approach for Tuning the SPR Peaks of Silver Nanoparticles. Polymers (Basel) [Internet]. 2017 Oct 4;9(12):486. Available from: <URL>.

12. Morimune S, Nishino T, Goto T. Poly(vinyl alcohol)/graphene oxide nanocomposites prepared by a simple eco-process. Polym J [Internet]. 2012 Oct 18;44(10):1056–63. Available from: <URL>.

13. Kharazmi A, Faraji N, Mat Hussin R, Saion E, Yunus WMM, Behzad K. Structural, optical, opto-thermal and thermal properties of ZnS–PVA nanofluids synthesized through a radiolytic approach. Beilstein J Nanotechnol [Internet]. 2015 Feb 23;6:529–36. Available from: <URL>.

14. Aslam M, Kalyar MA, Raza ZA. Fabrication of nano-CuO-loaded PVA composite films with enhanced optomechanical properties. Polym Bull [Internet]. 2021 Mar 21;78(3):1551–71. Available from: <URL>.

15. Ramesan MT, Jayakrishnan P, Anilkumar T, Mathew G. Influence of copper sulphide nanoparticles on the structural, mechanical and dielectric properties of poly(vinyl alcohol)/poly(vinyl pyrrolidone) blend nanocomposites. J Mater Sci Mater Electron [Internet]. 2018 Feb 28;29(3):1992–2000. Available from: <URL>.

16. Abdolrahimi M, Seifi M, Ramezanzadeh MH. Study the effect of acetic acid on structural, optical and mechanical properties of PVA/chitosan/MWCNT films. Chinese J Phys [Internet]. 2018 Feb;56(1):221–30. Available from: <URL>.

17. Zhang L, Yu P, Luo Y. Dehydration of caprolactam–water mixtures through cross-linked PVA composite pervaporation membranes. J Memb Sci [Internet]. 2007 Dec;306(1–2):93–102. Available from: <URL>.

18. Wu H, Xiao D, Lu J, Li T, Jiao C, Li S, et al. Preparation and Properties of Biocomposite Films Based on Poly(vinyl alcohol) Incorporated with Eggshell Powder as a Biological Filler. J Polym Environ [Internet]. 2020 Jul 4;28(7):2020–8. Available from: <URL>.

19. Koteswararao J, Satyanarayana SV, Madhu GM, Venkatesham V. Estimation of structural and mechanical properties of Cadmium Sulfide/PVA nanocomposite films. Heliyon [Internet]. 2019 Jun;5(6):e01851. Available from: <URL>.

20. Singh H, Kumar D, Sawant KK, Devunuri N, Banerjee S. Co-doped ZnO–PVA Nanocomposite for EMI Shielding. Polym Plast Technol Eng [Internet]. 2016 Jan 22;55(2):149–57. Available from: <URL>.